Available online at www.sciencedirect.com

ScienceDirect

IFAC-PapersOnline 58-24 (2024) i–vii

International Federation of Automatic Control

12th IFAC Symposium on Biological and Medical Systems BMS 2024

Villingen-Schwenningen, Germany, September 11-13, 2024

PROCEEDINGS

Edited by
Balázs Benyó
Budapest University of Technology and Economics, HU

ELSEVIER

IFAC Proceedings Volumes (IFAC-PapersOnline) — ISSN 2405-8963

IFAC PapersOnline — ISSN 2405-8963

Published by:
International Federation of Automatic Control (IFAC)
Hosting by Elsevier Ltd.

Available online at

www.sciencedirect.com

Publication date
September 2024

Copyright conditions

All publication material submitted for presentation at an IFAC-sponsored meeting (Congress, Symposium, Conference, Workshop) must be original and hence cannot be already published, nor can it be under review elsewhere. The authors take responsibility for the material that has been submitted. IFAC-sponsored conferences will abide by the highest standard of ethical behavior in the review process as explained on the Elsevier webpage (https://www.elsevier.com/authors/journal-authors/policies-and-ethics), and the authors will abide by the IFAC publication ethics guidelines (https://www.ifac-control.org/events/organizers-guide/PublicationEthicsGuidelines.pdf/view).

Accepted papers that have been presented at an IFAC meeting will be published in the proceedings of the event using the open-access IFAC-PapersOnLine series hosted on ScienceDirect (https://sciencedirect.com/). To this end, the author(s) must grant exclusive publishing rights to IFAC under a Creative Commons license when they submit the final version of the paper. The copyright belongs to the authors, who have the right to share the paper in the same terms allowed by the end user license, and retain all patent, trademark and other intellectual property rights (including research data).

(https://www.ifac-control.org/publications/copyright-conditions).

12th IFAC Symposium on Biological and Medical Systems
BMS 2024

Sponsored by

International Federation of Automatic Control (IFAC)
- Biological and Medical Systems, TC 8.2.

Co-Sponsored by

International Federation of Automatic Control (IFAC)
- TC 1.1. Modelling, Identification and Signal Processing
- TC 1.2. Adaptive and Learning Systems
- TC 2.1. Control Design
- TC 4.3. Robotics
- TC 8.4. Biosystems and Bioprocesses

International Programme Committee

Thomas Desaive, BE (IPC Chair)
Geoff Chase, NZ (IPC Co-Chair)
Marcos de Sales Guerra Tsuzuki, BR (IPC Vice-Chair from Industry)

Paul Docherty, NZ
Chris Pretty, NZ
Jennifer Knopp, NZ
Taous Meriem Laleg, FR
Chiew Yeong Shiong, MY
Kovács Levente, HU
László Szilágyi, RO
Antonio Ferramosca, IT
Olaf Simanski, DE
Teresa Mendonça, PT
Marcos de Sales Guerra Tsuzuki, BR
Thiago Martins, BR
Steffen Leonhardt, DE
Thomas Schauer, DE
Geoff Chase, NZ
Balázs Benyó, HU
Nicolai Spicher, DE
Philipp Rostalski, DE
Thomas Seel, DE
Georg Rauter, CH
Robert Riener, CH
Alberto Battistel, DE
Zhanqi Zhao, DE
Sabine Krüger-Ziolek, DE

National Organizing Committee

Knut Möller, DE (NOC Chair)
Thomas Schauer, DE (NOC Co-Chair)
Johannes Fallert, DE (NOC Vice-Chair from Industry)

IFAC-PapersOnline Editorial Board

FOREWORD

About three years ago, when the decision had been made to organize the 12th IFAC Symposium on Biological and Medical Systems in Villingen-Schwenningen, Germany, we were still uncertain about the long-term effects of the COVID-19 pandemic and feared that organizing scientific meetings on the traditional way will not be possible any more. Prof Knut Möller was optimistic and took the risk of organizing the main IFAC TC8.2-sponsored Symposium in whatever way it would be possible. Life was generous, and he was honored for his bravery, so the 12th IFAC BMS symposium happened to be the largest Symposium in the history of the BMS conferences!

Our Symposium, held every three years, has traditionally focused on applications of systems, modelling, informatics and control concepts, methodology and techniques in biology, physiology, medicine and healthcare. However, the submitted papers always reflect the actual societal and economic challenges faced all over the world to provide more productive medical treatment with the aid of engineering technologies, specifically using automation and control strategies and modelling techniques. Thus, following the previous editions in Berlin (2015), Sao Paulo (2018), and Ghent (2021), the 12th IFAC Symposium on Biological and Medical Systems stands under the sign of inter-disciplinarity.

Control, as the invisible thread of technology and its best application, has proved to be essential in service of humanity. Whether societal, economic, or simply instrumentation, control was always there. IFAC – The International Federation of Automatic Control – even in medicine, feels like the core for thousands of researchers who wish to address the great challenges ahead.

This landmark event has brought together contributions and scientific discussions from 155 academics, 20 research institutions and 9 medical technology companies across the world. More precisely, 611 authors from 32 countries, including 214 female contributors, reflecting our TC effort to strengthen the number of contributions from under-represented people and society.

Our 3-day event featured 7 invited tracks with 7 leading plenary speakers, one for each invited track, 60 invited papers and, altogether, 102 oral and 35 poster presentations distributed over 19 sessions. To strengthen industry connections, the majority of plenary keynote speakers represented significant industrial partners of the medical technology industry. As a novel concept the invited keynotes addressed and introduced the subsequent invited sessions. For the first time two invited sessions targeted application areas “Women’s Health” and “Mental Health”. A dedicated symposium session dealt with the recent advances in artificial intelligence (AI) in medicine, proving the rapid growth of AI-driven medical applications with measurable benefits. Medical signal processing and medical device technologies, as traditionally strong sessions of the meeting, included several innovative solutions for future industrial applications. The digital-twin technology was the focus of sessions dealing with physiological system modeling, introduced by an exciting keynote motivating the future potential of the technology. The increasing practical impact of artificial pancreas results was represented by two dedicated conference sessions. Showing the importance of the field, diabetes technology will be the main focus of the new TC 8.2 sponsored workshop organized in 2025. From the image processing and medical imaging sessions, a significant number of papers focused on investigating the opportunities of Electrical Impedance Tomography as a quickly improving imaging modality, which already has manufacturing support and has the potential to become one of the common diagnostic methods in intensive care.

A rigorous review by leading experts in the field guaranteed the high scientific quality of the conference. During the conference best paper, young author and best poster prices were awarded to outstanding contributions thanks to the financial support of industrial partners. The voluntary engagement of the members of the organizing committees, sponsors, associated editors, reviewers, and session chairs made this event possible. The participants enjoyed the hospitality of the Furtwangen University and the culture, art, and history of the city of Villingen-Schewnningen situated at the south-west ankle of Germany. We are convinced that IFAC BMS2024 was an inspiring experience for all the participants.

Balázs Benyó	Knut Möller	Thomas Desaive	Geoff Chase
Editor	NOC Chair	IPC Chair	IPC Co-Chair

Available online at www.sciencedirect.com

ScienceDirect

IFAC PapersOnLine CONFERENCE PAPER ARCHIVE

IFAC PapersOnLine 58-24 (2024) 257–262

Insulin on Board safety constraint effect in a CHoKI-based MPC for Artificial Pancreas

Beatrice Sonzogni * **José María Manzano** ** **Fabio Previdi** * **Antonio Ferramosca** *

* *Department of Management, Information and Production Engineering, University of Bergamo, Bergamo, Italy*

** *Department of Engineering, Universidad Loyola Andalucía, 41704 Dos Hermanas, Spain*

Abstract: This work presents a learning-based Model Predictive Control (MPC) algorithm for the artificial pancreas able to autonomously manage basal insulin injections in type 1 diabetic patients. The main goal is to keep the blood glucose levels within the euglycemic range (70-180 mg/dL), trying to avoid hypoglycemia. To prevent this event, additional constraints are added that consider the Insulin On Board (IOB). The data collection and the testing of the proposal are performed on the virtual patients of the FDA-accepted UVA/Padova simulator. The final results seem promising since the proposed controller reduces the time in hypoglycemia with respect to the standard constant basal insulin therapy.

Keywords: Artificial Pancreas, MPC, Learning-Based Control

1. INTRODUCTION

Type 1 Diabetes (T1D) is a chronic disease characterised by an excess of glucose in the blood, known as hyperglycemia (glucose levels higher than 180 mg/dL), caused by insufficient production of insulin (i.e. the hormone that regulates glucose levels). The therapy aims to restore and maintain the Blood Glucose (BG) level within the euglycemic range between 70 and 180 mg/dL, avoiding hypoglycemic events (i.e. BG below 70 mg/dL).

The standard therapy for T1D involves two types of external insulin administrations. The basal insulin infusion helps to maintain the glucose level within a safe range during fasting periods, while boluses of insulin are given to manage any increase in BG levels due to carbohydrate ingestion or to correct unexpected hyperglycemic events. The Artificial Pancreas is a device that improves the diabetes management, by employing a control algorithm to compute the insulin amounts to be delivered by a pump in a transcutaneous way, based on measures of glucose at the interstitial level provided by a sensor (Continuous Glucose Monitoring, CGM) (Toffanin et al., 2013). Model Predictive Control (MPC), one of the most widely used control algorithms for AP, optimises the control signal, by predicting the system's future evolution through a model, minimising a cost function and including constraints (Del Favero et al., 2019; Toffanin et al., 2013; Hovorka et al., 2004; Kovatchev, 2018; Boiroux et al., 2018; Abuin et al., 2020; González et al., 2020; Shi et al., 2018; Sun et al., 2022). However, since identifying a good model for a specific patient's glucose-insulin dynamics is difficult, data-driven methods are starting to acquire relevance in the field (Dutta et al., 2018; Paoletti et al., 2019).

In this work, the Componentwise Hölder Kinky Inference (CHoKI) method is exploited, a nonparametric learning technique that allows the building of robust MPCs that are stable by design (Manzano et al., 2021; Sonzogni et al., 2023). In this way, it is possible to exploit the subjects' data to make the BG prediction and use them inside an MPC to create a personalized controller. In addition, Insulin on Board (IOB) is also considered in the MPC construction. With the aim of reducing the risk of hypoglycemia, the amount of basal insulin is limited by the estimated IOB. To obtain the necessary data and to test the proposed control algorithm, the UVA/Padova simulator's virtual adult patients are used (The Epsilon Group, 2016). This simulator has been approved by the FDA as a substitute for preclinical trials (Man et al., 2014).

The layout of this note is as follows. In Section 2 the problem is presented, the CHoKI method is explained and applied to the T1D patient case. In Section 3 the MPC design and IOB constraint are explained. Section 4 shows the results of the proposed MPC applied on the UVA/Padova simulator, and Section 5 concludes the work.

Notation: A set of integers $[a, b]$ is denoted $\mathbb{I}_a^b$, $\mathbb{R}^n$ is the set of real vectors of dimension n and $\mathbb{R}^{n\times m}$ is the set of real matrices of dimension $n \times m$. M_i is the ith row of a matrix M. Given $v, w \in \mathbb{R}^{n_v}$, (v, w) implies $[v^T, w^T]^T$ and $v \leq w$ implies that the inequality holds for every component. $\|v\|$ is the Euclidean norm of v and $|v| = \{w : w_i = |v_i|, \forall i\}$. $A \ominus B$ denotes the Pontryagin difference and $A \times B$ the Cartesian product of the two sets A, B.

[1] This work was funded by the National Plan for NRRP Complementary Investments (PNC, established with the decree-law 6 May 2021, n. 59, converted by law n. 101 of 2021) in the call for the funding of research initiatives for technologies and innovative trajectories in the health and care sectors (Directorial Decree n. 931 of 06-06-2022) - project n. PNC0000003 - AdvaNced Technologies for Human-centrEd Medicine (project acronym: ANTHEM).

10.1016/j.ifacol.2024.11.046

$\mathbb{B}(v) = \{y : 0 \leq y \leq v\} \subset \mathbb{R}^{n_v}$ is the positive box of radius v and $\mathcal{B}(v) = \{y : |y| \leq v\} \subseteq \mathbb{R}^{n_v}$ is the ball of radius v. An n, m-dimensional matrix of ones is denoted $\mathbb{1}_{n\times m}$.

2. PROBLEM STATEMENT

According to what is proposed in Sonzogni et al. (2023), the insulin-glucose system of the patient can be explained as a continuous-time system, sampled every 5 min. The output $y(k) \in \mathbb{R}^{n_y}$ is the glucose level in mg/dL ($n_y = 1$) and there are two inputs ($n_u = 2$): u_1, the g of carbohydrates of the meals (not controllable) and the basal insulin in pmol (controllable). The boluses are assumed to be delivered as a function of the meals, thus they are not included in this model. A NARX model describes the connection between the output and the previous inputs and outputs, with the following state-space representation:

$$y(k+1) = f\big(x(k), u_1(k), u_2(k)\big) + e(k), \tag{1}$$

where the state $x \in \mathbb{R}^{n_x}$ is $x(k) = \big(y(k), \dots, y(k - n_a), u_1(k-1), \dots, u_1(k-n_b), u_2(k-1), \dots, u_2(k-n_c)\big)$, for some memory horizons $n_a, n_b, n_c \in \mathbb{N}_0$ (for the glucose, the meals and the basal insulin, respectively) and $e(k) \in \mathbb{R}^{n_y}$ is process noise. The arguments of f are aggregated into a vector $w = (x, u_1, u_2) \in \mathbb{R}^{n_w}$. Using this construction, a data set $\mathcal{D} = \{(w_k, y_{k+1})\}$ of $N_\mathcal{D}$ observations can be created, where $k = 1, \dots, N_\mathcal{D} - 1$.

2.1 CHoKI learning method

The Componentwise Hölder Kinky Inference (CHoKI) was introduced in Manzano et al. (2021). It is a learning method from the kinky inference class of learning approaches, that uses the Lipschitz interpolation, which is a technique based on the Hölder continuity of the function to be learned. Specifically, the CHoKI method is based on the componentwise Hölder continuity (see Definition 1).

Definition 1. Given the matrices $\mathcal{L}$ and $\mathcal{P} \in \mathbb{R}^{n_y \times n_w}$, a function $f : \mathcal{W} \to \mathcal{Y}$ is componentwise $\mathcal{L}$-$\mathcal{P}$-Hölder continuous if $\forall w_1, w_2 \in \mathcal{W}$ and $\forall i \in \mathbb{I}_1^{n_y}$

$$|f(w_1) - f(w_2)| \leq \mathfrak{d}_\mathcal{L}^\mathcal{P}(|w_1 - w_2|), \tag{2}$$

where $\mathfrak{d}_\mathcal{L}^\mathcal{P}(w) := (a : a_i = \sum_{j=1}^{n_w} \mathcal{L}_{i,j} w_j^{\mathcal{P}_{i,j}}, \forall i \in \mathbb{I}_1^{n_y})$.

This is done to determine the impact of each component of the regressor on each output. In this way, it is possible to consider that a function may have sudden changes along one input dimension while exhibiting smooth changes along another dimension. The value of the CHoKI predictor $\hat{f}(q; \Theta, \mathcal{D})$ for a query $q \in \mathbb{R}^{n_w}$ is computed as:

$$\begin{aligned}\hat{f}(q; \Theta, \mathcal{D}) = \frac{1}{2} \min_{i=1,\dots,N_\mathcal{D}} (\tilde{y}_i + \mathfrak{d}_\mathcal{L}^\mathcal{P}(|q - w_i|)) \\ + \frac{1}{2} \max_{i=1,\dots,N_\mathcal{D}} (\tilde{y}_i - \mathfrak{d}_\mathcal{L}^\mathcal{P}(|q - w_i|)),\end{aligned} \tag{3}$$

where $\Theta = \{\mathcal{L}, \mathcal{P}\}$, assuming that f is Hölder continuous and given a data set $\mathcal{D}$ of $N_\mathcal{D}$ observations. If the matrices Θ are unknown, they can be estimated by solving the following optimization problem offline:

$$\Theta = \arg\min_\Theta g(\Theta, \mathcal{D}_{\text{train}}, \mathcal{D}_{\text{test}}) \tag{4a}$$

$$\text{s.t. } |\tilde{y}_i - \tilde{y}_j| \leq \mathfrak{d}_\mathcal{L}^\mathcal{P}(|w_i - w_j|), \tag{4b}$$

$$\forall w_i, w_j \in \mathcal{W}_\mathcal{D}, w_i \neq w_j$$

$$0 < \mathcal{P}_{ij} \leq 1,\ \mathcal{L}_{ij} > 0, \quad i \in \mathbb{I}_1^{n_y}, j \in \mathbb{I}_1^{n_w}, \tag{4c}$$

Table 1. MPC settings

Adult	u_{ref} [pmol]	$N_\mathcal{D}$	$[L_a; L_b; L_c]$	μ [mg/dL]	N_c
#1	122.38	4769	[0.74; 5.46; 0.29]	14.83	2
#2	134.89	4946	[4.89; 3.96; 0.09]	10.19	2
#3	149.97	4985	[0.71; 5.45; 0.09]	9.29	3
#4	95.07	4768	[0.87; 9.94; 0.13]	8.19	3
#5	91.83	4149	[0.84; 5.52; 0.44]	13.91	2
#6	190.22	5334	[4.72; 3.52; 0.09]	11.27	1
#7	124.92	4804	[9.80; 0.9; 1.39]	11.89	1
#8	105.83	4698	[1.08; 5.84; 0.1]	7.8	3
#9	94.59	3976	[1.13; 4.09; 0.09]	11.63	2
#10	124.86	4961	[3; 2; 0.09]	10.1	1

where $\mathcal{W}_\mathcal{D}$ represents the input data points in $\mathcal{D}$, $\mathcal{D}_{\text{train}}$ and $\mathcal{D}_{\text{test}}$ are two disjoint data sets obtained splitting $\mathcal{D}$. The cost function to be minimized, being $\tilde{y}_i$ the measured values of $\mathcal{D}_{\text{test}}$ (Manzano et al., 2021), is:

$$g(\Theta, \mathcal{D}_{\text{train}}, \mathcal{D}_{\text{test}}) = \frac{1}{N_{\mathcal{D}_{\text{test}}}} \sum_{i=1}^{N_{\mathcal{D}_{\text{test}}}} \|\hat{f}(w_i; \Theta, \mathcal{D}_{\text{train}}) - \tilde{y}_i\|^2.$$

Then, the prediction model can be formulated in state-space as:

$$\begin{aligned}\hat{x}(k+1) &= \hat{F}\big(x(k), u_1(k), u_2(k)\big) \\ \hat{y}(k) &= M\hat{x}(k)\end{aligned} \tag{5}$$

where $\hat{F}\big(x(k), u_1(k), u_2(k)\big) = \big(\hat{f}(x(k), u_1(k), u_2(k)), y(k), \dots, y(k-n_a+1), u_1(k), \dots, u_1(k-n_b+1), u_2(k), \dots, u_2(k-n_c+1)\big)$ and $M = [I_{n_y}, 0, \dots, 0]$.

2.2 T1D patient case

To implement the CHoKI learning method, a data set has been created using the UVA/Padova simulator. Several simulations were performed on the virtual adult patients, modifying initial BG values, basal insulin amounts, and carbohydrate intakes (postprandial insulin boluses were also included), to get a proper space distribution of points in the input-output representation. This is crucial since the quality of the data set will impact the performance of both CHoKI predictions and the controller.

Once the data set is obtained, also the memory horizons n_a, n_b, n_c have to be identified. To do that, the combination that returned the lowest mean squared error between the predictions and the real values was selected using a cross-validation procedure, but the model complexity was also taken into consideration to avoid overfitting. The chosen orders were $n_a = 5$, $n_b = 9$ and $n_c = 3$.

To obtain the predictions employing (3), the hyperparameters $\Theta = \{\mathcal{L}, \mathcal{P}\}$ must be estimated solving the optimization problem (4). In this case, we have imposed $\mathcal{P} = \mathbb{1}_{n_y \times n_w}$, therefore the optimization problem is designed to obtain only the values of the matrix $\mathcal{L}$. We have also decided to estimate only three values: L_a for the glucose part, L_b for the meals, and L_c for the basal insulin. These are then repeated, to build $\mathcal{L} = [L_a \mathbb{1}_{n_a}; L_b \mathbb{1}_{n_b}; L_c \mathbb{1}_{n_c}] \in \mathbb{R}^{n_w}$.

To solve the optimization problem (4) the `fmincon` MATLAB function was used. The obtained results, reported in Table 1, are different for each virtual patient.

3. CHOKI-BASED ROBUST MPC

In this section, the CHoKI learning method is used to obtain open-loop glucose predictions, that are then used

inside the MPC. In this case, the control problem aims to maintain the BG level within the euglycemic zone, computing the right basal insulin amount (i.e. acting on the control action), and fulfilling input and output constraints. Specifically, the glucose should be maintained in the set $\mathcal{Y} = \{y : 55 \leq y \leq 300\,\text{mg/dL}\}$ and the basal insulin in the set $\mathcal{U} = \{u_2 : 0 \leq u_2 \leq 500\,\text{pmol}\}$.

The output constraints are tightened according to the error propagation, to ensure MPC robustness to differences between CHoKI predictions and real values. This way, the system in closed loop with the proposed controllers has been proven to be input-to-state stable (Manzano et al., 2021).

The set of tightened output constraints along the prediction horizon is given by

$$\mathcal{Y}_j = \mathcal{Y}_{j-1} \ominus \mathcal{R}_j, \quad j \in \mathbb{I}_1^N \tag{6}$$

where $\mathcal{Y}_0 = \mathcal{Y}$ and the reachability sets $\mathcal{R}_j$ account for the possible errors in the nominal predictions. This is computed as in (Manzano et al., 2021, Section III-A): the sets $\mathcal{M}_j$ and $\mathcal{G}_j$ can be calculated using the recursion $c_j = \mathfrak{d}_{\mathcal{L}}^{\mathcal{P}}(d_{j-1})$ and $d_j = (c_j, \ldots, c_{\sigma(j)}, 0, \ldots, 0)$, with $c_1 = \mu$, where $\mathcal{M}_j = \mathcal{B}(c_j)$ and $\mathcal{G}_j = \mathcal{B}(d_j)$. Then, $\mathcal{R}_j = \mathbb{B}(c_j)$. $\mu \in \mathbb{R}^{n_y}$, is the maximum absolute error obtained during the validation, such that $|y(k+1) - \hat{y}(1|k)| \leq \mu$. The computation is done just once and offline.

As in Sonzogni et al. (2023), it was noted that the extreme values of the possible deviation of the nominal prediction are highly improbable. Therefore, instead of using the maximum error, the value that represents the 90$^{\text{th}}$ percentile of the error distribution is used as μ (see Table 1). As some realizations may fall outside the 90$^{\text{th}}$ percentile range, some slack optimization variables $\boldsymbol{\delta} = \{\delta_{\min}, \delta_{\max}\}$ are introduced in the problem to prevent infeasibilities. Thus, starting from the $y_{\min}$ and $y_{\max}$ values from $\mathcal{Y}_j$ in (6), the new constraint is $\hat{y}(j|k) \in \mathcal{Y}_{j,\boldsymbol{\delta}}$, $\forall j \in \mathbb{I}_1^N$, where

$$\mathcal{Y}_{j,\boldsymbol{\delta}} = \{y : y_{\min}(j) - \delta_{\min}(j) \leq y \leq y_{\max}(j) + \delta_{\max}(j)\}. \tag{7}$$

This computation also determines the control horizon N_c, finding the maximum value that allows for a reasonable and non-empty set of tightened constraints. The CHoKI method may lead to short horizons, so a prediction horizon N_p longer than the control horizon is implemented, to improve the controller's predictive ability and domain of attraction. Thus, a local control is defined for the inputs from N_c to N_p, namely: $u = K(\overline{x} - x) + \overline{u}$. Where $K \in \mathbb{R}^{n_u \times n_x}$ is the Linear Quadratic Regulator (LQR) gain, and $(\overline{x}, \overline{u})$ is the equilibrium point around which the system $\hat{F}(x, u)$ is linearized (i.e. $x(k+1) = Ax(k) + Bu(k)$, $u = (u_1, u_2)$). Specifically, $\overline{x}$ contains $\overline{y} = 120\,\text{mg/dL}$ and $\overline{u} = (0, u_{\text{ref}})$. The matrices $A \in \mathbb{R}^{n_x \times n_x}$ and $B \in \mathbb{R}^{n_x \times n_u}$ are numerically computed with the input-output data, as in Sonzogni et al. (2023).

3.1 Insulin On Board estimation

The IOB represents the insulin currently active in the body, which is influenced by the patient's metabolism and the Insulin Action Duration (DIA). This dynamic value can be considered as an upper constraint in the MPC optimization problem, to limit the maximum value of basal insulin, and thus to reduce the risk of hypoglycemic events.

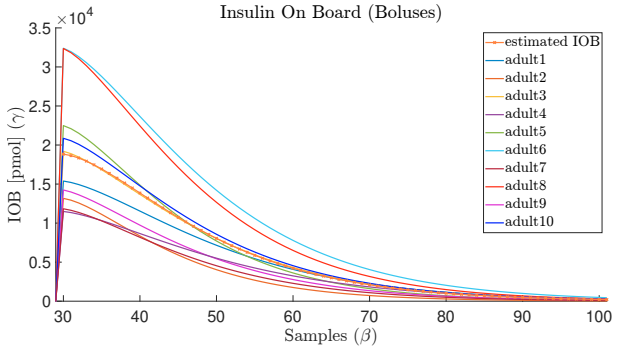

Fig. 1. Each line represents the real IOB of a specific patient, coming from the simulator. The orange line is for the estimated IOB.

At each sampling time k the IOB can be estimated by analysing the residuals of the past bolus insulin administration, which means having:

$$IOB(k) = \textstyle\sum_{i=1}^{n_{IOB}} \alpha(k-i) u_b(k-i), \tag{8}$$

in which the vector of weights, denoted by α, represents the insulin action curve, while u_b contains the previous insulin boluses injections. n_{IOB} is the DIA, considered with a sampling time of 5 min, and in this case, looking at the data coming from the simulator, it is chosen to be $n_{IOB} = 72$, which means 6 h (León-Vargas et al., 2013).

The value of the upper limit for the calculation of the basal dose is $u_2^{\max}$ and it is derived from

$$u_2^{\max}(k+j) = \begin{cases} u_2^{\lim} - IOB(k+j) & \text{if } u_2^{\lim} > IOB(k+j) \\ u_{\text{ref}} & \text{otherwise} \end{cases}$$

where k is the sampling time and $j \in \mathbb{I}_0^{N_p-1}$ (Ellingsen et al., 2009). The maximum amount of basal insulin that can be delivered is $u_2^{\lim} = 500\,\text{pmol}$. u_{ref} is the basal insulin reference value, which is the constant basal insulin dose continuously delivered for each virtual patient by the UVA/Padova simulator for the standard therapy. The IOB varies at each step along the prediction horizon (i.e. with j), and thus the estimations have to decrease according to the insulin action curve, without considering possible new boluses, since the meals are unpredictable. Thus, the new set for the basal insulin amount u_2 is

$$\mathcal{U}_2 = \{u_2 : 0 \leq u_2 \leq u_2^{\max}\}. \tag{9}$$

In Sonzogni et al. (2024), a linear weight decreasing from 1 to 0 is tested, which leads to a very conservative result, due to the overestimation of the IOB values. Therefore, in this work, the weights of the insulin action curve α are computed by exploiting the data coming from the simulator. Specifically, to get the IOB decreasing behavior, the following sum of two exponential functions is considered: $\gamma_m = a_m e^{b_m \beta} + c_m e^{d_m \beta}$, where the parameters a_m, b_m, c_m and d_m have to be estimated from the data (β, γ), where β is the time and γ is the IOB value. The estimated parameters were obtained considering the IOB curves of the analysed patient. The results are: $a_m = 8.2 \cdot 10^5$, $b_m = -0.08$, $c_m = -1.3 \cdot 10^6$ and $d_m = -0.11$, visible in Figure 1. After that, to get the weights $\alpha \in \mathbb{R}^{n_{IOB}}$ that have to be multiplied to u_b, the values γ_m are normalized between 0 and 1, to follow the real IOB behavior.

Figure 2 displays an example of the IOB estimation for virtual Adult 10. This shows that (8) approximates quite

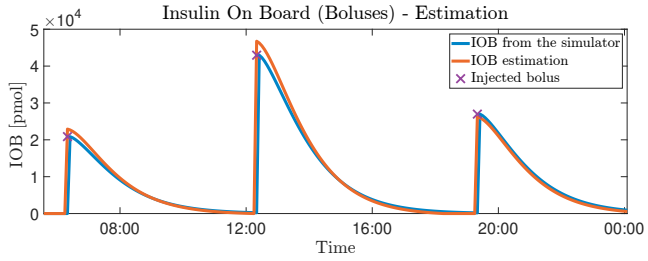

Fig. 2. The orange line represents the estimated IOB, the blue one the IOB computed by the simulator and the injected boluses are the purple crosses. This is an example of the virtual patient Adult 10.

well the real values and the choice of DIA equal to 6 h is appropriate. After a bolus, the initial IOB value might differ between the two curves. This is because the estimated IOB value is based on the calculated value of the bolus for the meal. While the real IOB value is based on the value actually injected, which may vary from the calculated value due to pump noise.

To prevent infeasibilities during MPC resolution, N_p slack variables δ_u were included in the optimization problem. These were added to the upper bound $u_2^{\max}$ in equation (9), obtaining $\forall j \in \mathbb{I}_0^{N_p-1}$:

$$\mathcal{U}_2' = \{u_2(j) : 0 \le u_2(j) \le u_2^{\max}(j) + \delta_u(j)\}. \tag{10}$$

3.2 Optimization problem

In this section the optimization problem is presented, including also the IOB in the constraints (see (11f)), following the idea proposed in Sonzogni et al. (2024). The N_c resulting from the tightened constraints for each virtual patient are in Table 1. To obtain at least 60 minutes of predictions, the prediction horizon is set to $N_p = 12$.

The MPC optimization problem is set as follows:

$$\min_{u_2, y_a, \delta_{\text{hyper}}, \delta_{\text{hypo}}, \boldsymbol{\delta}, \delta_u} V_N(\hat{x}, u; \Theta, \mathcal{D}) \tag{11a}$$

$$\text{s.t. } \hat{x}(0|k) = x(k) \tag{11b}$$

$$\hat{x}(j+1|k) = \hat{F}(\hat{x}(j|k), u_1(j), u_2(j)),\ j \in \mathbb{I}_0^{N_c-1} \tag{11c}$$

$$\hat{x}(j+1|k) = \hat{F}(\hat{x}(j|k), K(\bar{x} - x(j)) + \bar{u}),\ j \in \mathbb{I}_{N_c}^{N_p-1} \tag{11d}$$

$$\hat{y}(j|k) = M\hat{x}(j|k),\ j \in \mathbb{I}_0^{N_p-1} \tag{11e}$$

$$u_2(j) \in \mathcal{U}_2',\ j \in \mathbb{I}_0^{N_p-1}, \tag{11f}$$

$$\hat{y}(j|k) \in \mathcal{Y}_{j,\boldsymbol{\delta}},\ j \in \mathbb{I}_0^{N_c-1} \tag{11g}$$

$$\hat{y}(j|k) \in \mathcal{Y}_{N_c,\boldsymbol{\delta}},\ j \in \mathbb{I}_{N_c}^{N_p-1} \tag{11h}$$

$$u_1(j) = 0,\ j \in \mathbb{I}_1^{N_p-1} \tag{11i}$$

$$70 - \delta_{\text{hypo}} \le y_a \le 140 + \delta_{\text{hyper}};\ \delta_{\text{hyper}}, \delta_{\text{hypo}} \ge 0 \tag{11j}$$

$$\delta_{\min}(j), \delta_{\max}(j), \delta_u(j) \ge 0,\ j \in \mathbb{I}_0^{N_p-1} \tag{11k}$$

where $\mathcal{Y}_{j,\boldsymbol{\delta}}$ and $\mathcal{Y}_{N_c,\boldsymbol{\delta}}$ come from (7), (11i) is used because meals are unpredictable, y_a is the setpoint, which is an auxiliary optimization variable, for implementing the MPC in a zone control fashion, and $u = (u_1, u_2)$.

The cost function is a summation of different components:

$$V_N(\hat{x}, u; \Theta, \mathcal{D}) = V_{N_c} + V_{N_p} + V_s + \lambda V_P + V_\delta + V_u. \tag{12}$$

The first ones are the stage costs, along N_c and N_p:

$$V_{N_c} = \textstyle\sum_{j=0}^{N_c-1} \|\hat{y}(j|k) - y_a\|_Q^2 + \|u_2(j) - u_{\text{ref}}\|_R^2, \tag{13}$$

$$V_{N_p} = \textstyle\sum_{j=N_c}^{N_p-1} \|\hat{y}(j|k) - y_a\|_Q^2. \tag{14}$$

The chosen weights are $R = 10$ and $Q = 100$ for Adult number 8 and 9 and $Q = 1$ for the others.
The terminal cost, usually considered for MPC stability:

$$V_P = \|\hat{x}(N_p|k) - x_{\text{ref}}\|_P^2, \tag{15}$$

where x_{ref} is the reference state (with y_a, no meals and u_{ref}). P is the Riccati equation solution, given the LQR control gain K for the linearised system around the reference point. As no terminal constraint is taken into account, V_P is weighted by a factor $\lambda = 10$.
Other costs are added to penalise the slack variables used in the constraints (i.e. $\delta_{\text{hypo}}, \delta_{\text{hyper}}, \boldsymbol{\delta}, \delta_u$):

$$V_s = p_{\text{hyper}}\delta_{\text{hyper}}^2 + p_{\text{hypo}}\delta_{\text{hypo}}^2, \tag{16}$$

$$V_\delta = \textstyle\sum_{j=1}^{N_P} \|\delta_{\min}(j)\|_{p_{\min}}^2 + \|\delta_{\max}(j)\|_{p_{\max}}^2, \tag{17}$$

$$V_u = \textstyle\sum_{j=1}^{N_p} \|\delta_u(j)\|_{p_u}^2, \tag{18}$$

where p_{hypo} is greater than p_{hyper} and $p_{\min}$ greater than $p_{\max}$ to represent that hypoglycemia is more dangerous than hyperglycemia (i.e. $p_{\text{hypo}} = p_{\min} = 1 \cdot 10^7$, $p_{\text{hyper}} = p_{\max} = 1 \cdot 10^6$), and $p_u = 1 \cdot 10^7$ (Abuin et al., 2020).

4. RESULTS

The proposed control algorithm was implemented in the UVA/Padova simulator. Simulations of three days were conducted on virtual adult patients to test the algorithm, considering three meals per day, each lasting 15 min and with boluses given by the simulator 20 minutes after each meal. Specifically, 20 g at 06:00am, 90 g at 12:00pm, and 30 g at 07:00pm for the first day, 30 g at 07:00am, 80 g at 12:30pm, and 50 g at 08:00pm for the second day, and 40 g at 06:30am, 100 g at 01:00pm, and 60 g at 07:30pm for the last day. The simulation settings are the same as those used for the data collection.
In Figure 3, the upper part shows the BG trends of the virtual patients, resulting from the insulin injections reported in the lower part. The BG values mainly fall within the euglycemic range (i.e. between 70 and 180 mg/dL, green zone); they rise after the meals (indicated by black triangles). The controller was designed with the IOB constraint to avoid hypoglycemic events, thus this result is achieved, even if we obtain a conservative controller.
To better evaluate the quality of closed-loop glucose control, additional tools can be considered: Time In Range (TIR), Control-Variability Grid Analysis (CVGA) and Glycemia Risk Index (GRI). The TIR represents the proportion of time that a patient's BG level stays within a specific range (Battelino et al., 2019). In Table 2, the TIR results indicate that the proposed controller tends to be conservative, allowing a bit of hyperglycemia to avoid hypoglycemia: although the percentage of time spent in hyperglycemic ranges is slightly higher than expected, the patients never enter the hypoglycemic ranges. The CVGA is a visualization technique used to represent a patient's extreme glucose excursions. It is done by plotting the minimum and maximum BG values of a patient on the x and y-axis, respectively. Each patient is represented as a point in a plane that is divided into nine regions corresponding

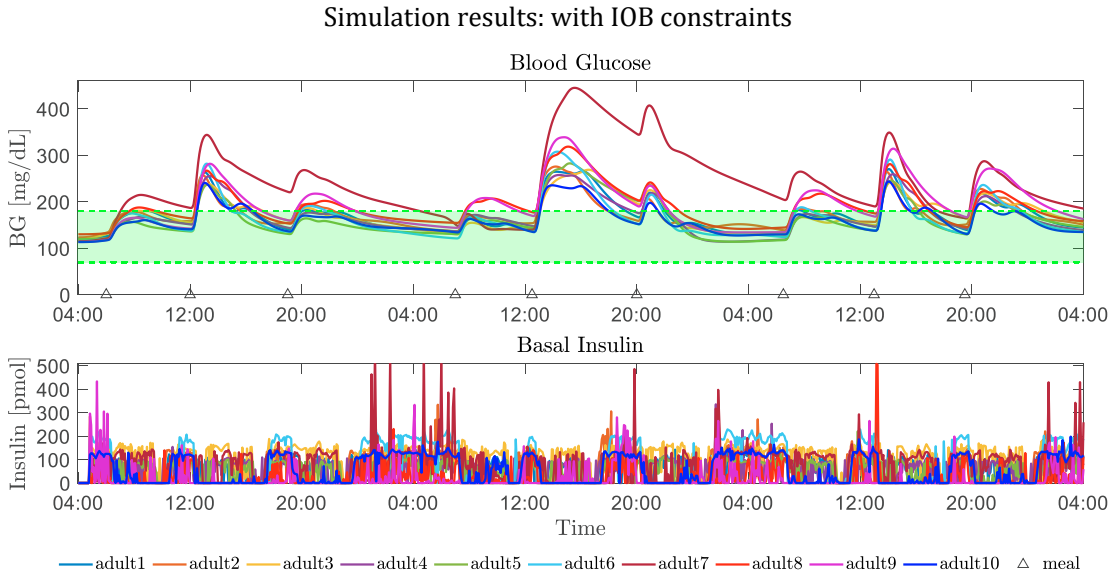

Fig. 3. The upper plot displays the BG trend of each subject. The green zone represents the euglycemic range, and the black triangles indicate meal times. The lower plot shows the basal insulin computed by the proposed controller.

to different levels of glycemic control quality (Magni et al., 2008). As shown in Figure 4a, most patients are in the safe zones, except for virtual adults 7, 8 and 9 who are in the Upper C zone due to their high BG maximum values. The GRI is a score, ranging from 0 to 100, that reflects both the risk of hyperglycemia and of hypoglycemia (Klonoff et al., 2022). It is calculated by combining the two components: $GRI = \big(3.0(TBR_2 + 0.8\,TBR_1)\big) + \big(1.6(TAR_2 + 0.5\,TAR_1)\big)$, where TBR_2 is the percentage of time in which the subject's BG is below 54 mg/dL, TBR_1 for the BG between 54 and 70 mg/dL, TAR_1 for the BG between 180 and 250 mg/dL and TAR_2 for BG above 250 mg/dL. The first part is the hypoglycemic component (represented on the x-axis) and the second is the hyperglycemic one (represented on the y-axis). In Figure 4b all the dots lay on the y-axis due to the controller design: the aim is to avoid hypoglycemic events, thus the higher risk component is the hyperglycemic one.

This controller results to be too conservative for adult 7, who remains in a hyperglycemic state for too long. Thus, additional analysis is required to enhance the control, also due to the patient's high variability and complex response to insulin.

To be compared with the results reported in Sonzogni et al. (2024), obtained using linear weights in the IOB estimation, the proposed controllers are applied to the same patients with the same simulation settings. Figure 5 compares the mean and standard deviation of the BG values of the virtual subjects in both cases. The controller proposed here shows less conservative results. Figure 6 shows that the IOB values computed with the linear weights (green line) overestimate the real values (blue line), while the exponential weights allow to obtain better estimates of the IOB values (orange line).

5. CONCLUSION

The AP requires a control algorithm able to compute the appropriate amount of basal insulin, to keep the BG of T1D patients inside the safe range. In this work, an MPC

Table 2. TIR percentages

Adult	<54 mg/dL	54-70 mg/dL	70-180 mg/dL	180-250 mg/dL	>250 mg/dL
# 1	0%	0%	72%	21%	7%
# 2	0%	0%	71%	24%	5%
# 3	0%	0%	64%	32%	4%
# 4	0%	0%	74%	21%	5%
# 5	0%	0%	75%	20%	5%
# 6	0%	0%	75%	18%	7%
# 7	0%	0%	20%	45%	35%
# 8	0%	0%	47%	44%	9%
# 9	0%	0%	47%	39%	14%
# 10	0%	0%	80%	20%	0%

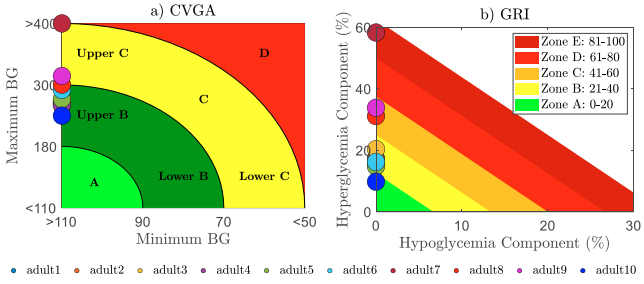

Fig. 4. a) Control-Variability Grid Analysis results. b) Glycemia Risk Index results.

based on the CHoKI learning method is proposed as a controller. It considers also the IOB, estimating its values with exponential weights, that were obtained from data coming from the UVA/Padova simulator. This is done to limit the basal insulin amount, so as to avoid hypoglycemic events, due to their dangerousness.

The controller is then tested on the virtual patients of the simulator. The results seem promising, since the IOB constraints prevent the subjects from entering the hypoglycemic range. The exponential weights in the IOB estimation perform better than the linear one, however, the controller might still be too conservative, allowing some hyperglycemic events.

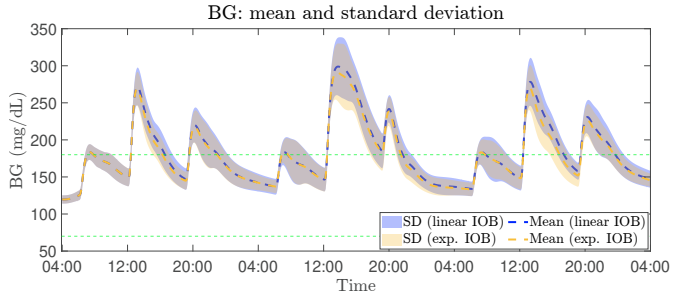

Fig. 5. Comparison of the BG: the simulations with linear IOB are in blue, and the exponential ones in yellow.

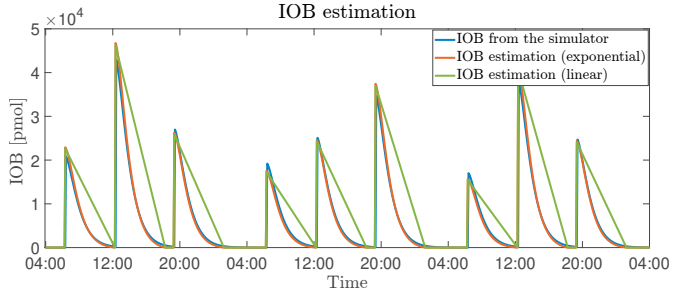

Fig. 6. The estimated boluses IOB with exponential weights are represented as the orange line, the one with linear weights is the green line, and the one of the simulator is in blue (Adult 10 example).

REFERENCES

Abuin, P., Rivadeneira, P.S., Ferramosca, A., and González, A.H. (2020). Artificial pancreas under stable pulsatile MPC: Improving the closed-loop performance. *Journal of Process Control*, 92, 246–260.

Battelino, T., Danne, T., Bergenstal, R.M., Amiel, S.A., Beck, R., Biester, T., Bosi, E., Buckingham, B.A., Cefalu, W.T., Close, K.L., et al. (2019). Clinical targets for continuous glucose monitoring data interpretation: recommendations from the international consensus on time in range. *Diabetes care*, 42(8), 1593–1603.

Boiroux, D., Bátora, V., Hagdrup, M., Wendt, S.L., Poulsen, N.K., Madsen, H., and Jørgensen, J.B. (2018). Adaptive model predictive control for a dual-hormone artificial pancreas. *Journal of Process Control*, 68, 105–117.

Del Favero, S., Toffanin, C., Magni, L., and Cobelli, C. (2019). Deployment of modular MPC for type 1 diabetes control: the Italian experience 2008–2016. In *The Artificial Pancreas*, 153–182. Elsevier.

Dutta, S., Kushner, T., and Sankaranarayanan, S. (2018). Robust data-driven control of artificial pancreas systems using neural networks. In *Computational Methods in Systems Biology: 16th International Conference, CMSB 2018, Brno, Czech Republic, September 12-14, 2018, Proceedings 16*, 183–202. Springer.

Ellingsen, C., Dassau, E., Zisser, H., Grosman, B., Percival, M.W., Jovanovič, L., and Doyle III, F.J. (2009). Safety constraints in an artificial pancreatic β cell: an implementation of model predictive control with insulin on board. *Journal of diabetes science and technology*, 3(3), 536–544.

González, A.H., Rivadeneira, P.S., Ferramosca, A., Magdelaine, N., and Moog, C.H. (2020). Stable impulsive zone model predictive control for type 1 diabetic patients based on a long-term model. *Optimal Control Applications and Methods*, 41(6), 2115–2136.

Hovorka, R., Canonico, V., Chassin, L.J., Haueter, U., Massi-Benedetti, M., Federici, M.O., Pieber, T.R., Schaller, H.C., Schaupp, L., Vering, T., et al. (2004). Nonlinear model predictive control of glucose concentration in subjects with type 1 diabetes. *Physiological measurement*, 25(4), 905.

Klonoff, D.C., Wang, J., Rodbard, D., Kohn, M.A., Li, C., Liepmann, D., Kerr, D., Ahn, D., Peters, A.L., Umpierrez, G.E., et al. (2022). A glycemia risk index (GRI) of hypoglycemia and hyperglycemia for continuous glucose monitoring validated by clinician ratings. *Journal of diabetes science and technology*, 19322968221085273.

Kovatchev, B. (2018). Automated closed-loop control of diabetes: the artificial pancreas. *Bioelectronic Medicine*, 4(1), 1–12.

León-Vargas, F., Garelli, F., De Battista, H., and Vehí, J. (2013). Postprandial blood glucose control using a hybrid adaptive PD controller with insulin-on-board limitation. *Biomedical Signal Processing and Control*, 8(6), 724–732.

Magni, L., Raimondo, D.M., Man, C.D., Breton, M., Patek, S., De Nicolao, G., Cobelli, C., and Kovatchev, B.P. (2008). Evaluating the efficacy of closed-loop glucose regulation via control-variability grid analysis. *Journal of diabetes science and technology*, 2(4), 630–635.

Man, C.D., Micheletto, F., Lv, D., Breton, M., Kovatchev, B., and Cobelli, C. (2014). The UVA/PADOVA type 1 diabetes simulator: new features. *Journal of diabetes science and technology*, 8(1), 26–34.

Manzano, J.M., Muñoz de la Peña, D., Calliess, J.P., and Limon, D. (2021). Componentwise Hölder Inference for Robust Learning-Based MPC. *IEEE Trans. On Automatic control*, 66(11), 5577–5583.

Paoletti, N., Liu, K.S., Chen, H., Smolka, S.A., and Lin, S. (2019). Data-driven robust control for a closed-loop artificial pancreas. *IEEE/ACM trans. on computational biology and bioinformatics*, 17(6), 1981–1993.

Shi, D., Dassau, E., and Doyle, F.J. (2018). Adaptive zone model predictive control of artificial pancreas based on glucose-and velocity-dependent control penalties. *IEEE Trans. on Biomedical Engineering*, 66(4), 1045–1054.

Sonzogni, B., Manzano, J.M., Polver, M., Previdi, F., and Ferramosca, A. (2023). CHoKI-based MPC for blood glucose regulation in artificial Pancreas. *IFAC-PapersOnLine*, 56(2), 9672–9677.

Sonzogni, B., Manzano, J.M., Polver, M., Previdi, F., and Ferramosca, A. (2024). CHoKI-based MPC for blood glucose regulation in Artificial Pancreas. *arXiv preprint arXiv:2401.17157*.

Sun, X., Rashid, M., Hobbs, N., Brandt, R., Askari, M.R., and Cinar, A. (2022). Incorporating prior information in adaptive model predictive control for multivariable artificial pancreas systems. *Journal of Diabetes Science and Technology*, 16(1), 19–28.

The Epsilon Group (2016). DMMS.R (Version 1.1) [Software]. Retrieved from https://tegvirginia.com/.

Toffanin, C., Messori, M., Di Palma, F., De Nicolao, G., Cobelli, C., and Magni, L. (2013). Artificial pancreas: model predictive control design from clinical experience.